PERGAMON

International Journal of Heat and Mass Transfer 46 (2003) 333–339

International Journal of HEAT and MASS TRANSFER

www.elsevier.com/locate/ijhmt

Use of the microscopic parabolic heat conduction model in place of the macroscopic model validation criterion under harmonic boundary heating

M.A. Al-Nimr *, M. Hader, M. Naji

Department of Mechanical Engineering, Jordan University of Science and Technology, P.O. Box 3030, Irbid 22110, Jordan

Received 11 December 2001; received in revised form 5 April 2002

Abstract

Parabolic heat conduction models are considered. The validity of using a microscopic under harmonic fluctuating boundary heating source is investigated. It is found that using the microscopic parabolic heat conduction model is essential when $\bar{\omega}C_l/G > 0.1$. The phase-shift between the electron gas and solid lattice temperatures is found to be $\tan^{-1}(\bar{\omega}C_l/G)$. This phase-shift reaches a fixed value of 1.5708 rad at very large values of $\bar{\omega}C_l/G$. It is found that using the microscopic parabolic heat conduction model is essential when $\bar{\omega} > 1 \times 10^9$ rad/s for most metallic layers regardless of their thickness.

Keywords: Microscopic heat conduction; Parabolic microscopic model; Two-step heat conduction model; Parabolic two-step heat conduction model; Microscopic and macroscopic heat conduction

1. Introduction

Energy transport during high-rate heating of thin metal films is a rapidly emerging area in heat transfer [1–13]. When a thin film is exposed to a very rapid heating process, such that induced by a short-pulse laser, the response time of the film is typically of the order of 1 ps, which is comparable to the phonon–electron thermal relaxation time. Under these situations, thermal equilibrium between solid lattice and electron gas cannot be assumed and heat transfer in the electron gas and the metal lattice needs to be considered separately. Models describing the non-equilibrium thermal behavior in such cases are called the microscopic two-step models. Two microscopic heat conduction models are available in the literature. The first one is the parabolic two-step model [1–5,8–10] and the second one is the hyperbolic two-step model [1,3,7,11].

Ultrafast heating of metals consists of two major steps of energy transfer that occur simultaneously. In the first step, electrons absorb most of the incident radiation energy and the excited electron gas transmits its energy to the lattice through inelastic electron–phonon scattering process [1,3]. In the second step, the incident radiation absorbed by the metal film diffuses spatially within the film mainly by the electron gas. For typical metals, depending on the degree of electron–phonon coupling, it takes about 0.1–1 ps for electrons and lattice to reach thermal equilibrium. When the ultrafast heating pulse duration is comparable with or less than this thermalization time, electrons and lattice are not in thermal equilibrium.

In the literature, numerous works have been conducted using the microscopic parabolic heat conduction model [8–10,14,15]. These works refer that using this model is a necessity in applications involving very thin films and very short duration heating sources. In the present work, we intend to investigate the thermal

* Corresponding author. Tel.: +962-2-295-111x2546; fax: +962-2-295-123.
E-mail address: malnimr@just.edu.jo (M.A. Al-Nimr).

0017-9310/03/$ - see front matter © 2002 Elsevier Science Ltd. All rights reserved.
PII: S0017-9310(02)00263-6

Nomenclature

A	dimensionless quantity, GL^2/k_e
C	heat capacity (J/m^3 K)
C_R	heat capacity ratio, C_e/C_l
G	electron–phonon coupling factor (W/m^3 K)
i	imaginary number, $\sqrt{-1}$
k_e	electron gas thermal conductivity (W/m K)
$2L$	film thickness (m)
t	time (s)
T	temperature (K)
T_0	amplitude of harmonic fluctuating temperature (K)
$W(\zeta)$	spatial amplitude of the temperature
x	transverse coordinate (m)

Greek symbols

ε	relative amplitude of oscillations
η	dimensionless time, tk_e/C_eL^2
θ	dimensionless temperature, $(T-T_0)/T_0$
ζ	dimensionless axial coordinate, x/L
$\bar{\omega}$	angular velocity of fluctuating temperature (rad/s)
ω	dimensionless angular velocity of fluctuating temperature, $\bar{\omega}C_eL^2/k_e$

Subscripts

e	electron gas
l	solid lattice
R	ratio

behavior of metal films under the effect of a harmonic fluctuating heating source applied at the film boundary. The heating source will heat the electron gas, which in turn exchange part of its energy with the solid lattice. In applications involving heating sources with very high frequency, there is no enough time available for the electron gas and solid lattice to attain the same temperature. The goal of the present work is to investigate the conditions under which using the microscopic parabolic heat conduction model in place of the macroscopic heat conduction model is a necessity.

2. Analysis

Consider a plate of thickness $2L$, where the boundaries of the plate are subjected to an imposed temperature that fluctuates in a harmonic manner. The frequency of fluctuations is very high so that using the microscopic heat conduction model becomes important. The governing equations describing the film thermal behavior under these conditions are given as [1]:

$$C_e\frac{\partial T_e}{\partial t} = k_e\frac{\partial^2 T_e}{\partial x^2} - G(T_e - T_l) \tag{1}$$

$$C_l\frac{\partial T_l}{\partial t} = G(T_e - T_l) \tag{2}$$

The boundary conditions are given as:

$$\frac{\partial T_e}{\partial x}(t,0) = 0, \quad T_e(t,L) = T_0(1+\varepsilon\sin\bar{\omega}t) \tag{3}$$

where ε and $\bar{\omega}$ are, respectively, the amplitude and angular velocity of the fluctuating temperature imposed on the boundaries.

Now using the dimensionless parameters defined in the nomenclature. Eqs. (1)–(3) are reduced to:

$$\frac{\partial\theta_e}{\partial\eta} = \frac{\partial^2\theta_e}{\partial\zeta^2} - A(\theta_e - \theta_L) \tag{4}$$

$$\frac{\partial\theta_l}{\partial\eta} = C_RA(\theta_e - \theta_l) \tag{5}$$

$$\frac{\partial\theta_e}{\partial\zeta}(\eta,0) = 0, \quad \theta_e(\eta,1) = \varepsilon\sin\omega\eta = \varepsilon\mathrm{Im}\{e^{i\omega\eta}\} \tag{6}$$

Also,

$$A = \frac{GL^2}{k_e}, \quad C_R = \frac{C_e}{C_l}, \quad \omega = \bar{\omega}\frac{C_eL^2}{k_e}.$$

Eqs. (4)–(6) assume solutions in the form:

$$\begin{aligned}\theta_e(\eta,\zeta) &= \mathrm{Im}\{W_e(\zeta)e^{i\omega\eta}\}\\ \theta_l(\eta,\zeta) &= \mathrm{Im}\{W_l(\zeta)e^{i\omega\eta}\}\end{aligned} \tag{7}$$

Substitute Eq. (7) into Eqs. (4)–(6) yields:

$$i\omega W_e = \frac{d^2W_e}{d\zeta^2} - A(W_e - W_l) \tag{8}$$

$$i\omega W_l = C_RA(W_e - W_l) \tag{9}$$

$$\frac{dW_e}{d\zeta}(0) = 0, \quad W_e(1) = \varepsilon \tag{10}$$

Eqs. (8)–(10) are decoupled and solved to yield:

$$W_e(\zeta) = \varepsilon\frac{\cosh\lambda\zeta}{\cosh\lambda} \tag{11}$$

$$W_l(\zeta) = M\varepsilon\frac{\cosh\lambda\zeta}{\cosh\lambda} \tag{12}$$

with

$$M = \frac{C_RA}{i\omega + C_RA} \tag{13}$$

and

$$\lambda = \sqrt{A + \mathrm{i}\omega - AM}$$

Eq. (13) may be rewritten as:

$$M = \frac{C_R A}{\sqrt{\omega^2 + C_R^2 A^2}} e^{-\mathrm{i}\delta} \tag{14}$$

with

$$\delta = \tan^{-1}\left(\frac{\omega}{C_R A}\right) \tag{15}$$

where δ represents the phase-shift between electron gas and solid lattice temperatures.

A comparison between Eqs. (11) and (12) reveals that using the macroscopic parabolic heat conduction model is possible if

$$M \approx 1 \tag{16}$$

Table 1
Angular frequencies beyond which using the microscopic model is essential

Metal	$\bar{\omega} \geqslant$ (rad/s)	A	C_R	$G \times 10^{16}$ (W/m^3 K)
Cu	1.4×10^9	124.352	0.006176	4.8
Ag	1.12×10^9	66.826	0.00084	2.8
Pb	8.27×10^9	3542.86	0.014	12.4

It will be assumed that if condition (16) is satisfied within a 1% deviation, then the macroscopic heat conduction model is satisfied. In this case, $T_e \approx T_l \approx T$ and Eqs. (1) and (2) become:

$$(C_e + C_l)\frac{\partial T}{\partial t} = k\frac{\partial^2 T}{\partial x^2} \tag{17}$$

which is the classical macroscopic parabolic heat conduction model. If the deviation in Eq. (16) is more than 1%, then using the microscopic heat conduction model is essential. To validate the use of the macroscopic heat conduction model in layers exposed to a harmonic fluctuating boundary heating source, Eqs. (14)–(16) imply, with less than 1% deviation between the macroscopic and the microscopic models, that:

$$\frac{\omega}{C_R A} < 0.1 \tag{18}$$

In terms of the dimensional properties, Eq. (18) is rewritten as:

$$\frac{\bar{\omega} C_l}{G} < 0.1 \tag{19}$$

Criterion (19) implies that the macroscopic heat conduction model under the effect of fluctuating boundary heating source may be used in applications having small frequencies $\bar{\omega}$, small lattice thermal capacity C_l and large coupling factors G.

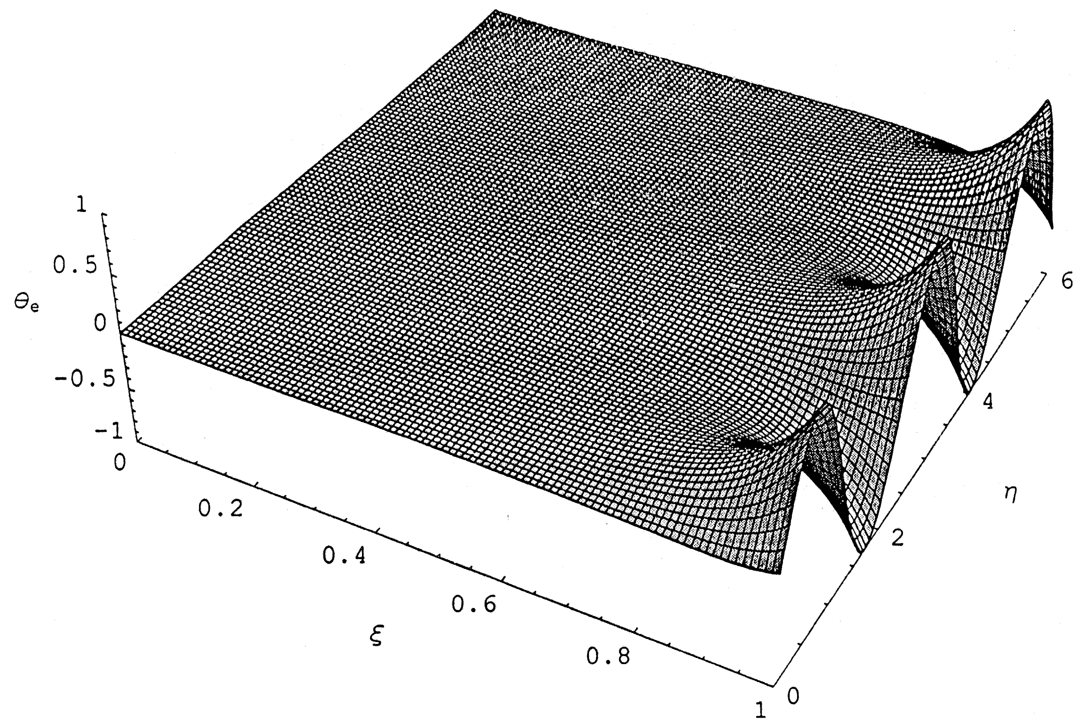

Fig. 1. Spatial and transient electron gas temperature distribution for Cu ($A = 124.352$, $C_R = 0.0061765$, $\bar{\omega} = 5 \times 10^5$, $\varepsilon = 1.0$).

Fluctuating heating sources with small frequencies gives the electron gas enough time to transmit its high energy to the solid lattice. Small lattice thermal capacity implies that solid lattice needs small energy to attain the same temperature as the electron gas and this in turn shortens the time required by both the lattice and the electron to attain the thermal equilibrium state. Large coupling factors G enhances the energy exchange process between electron gas and solid lattice and this also shortens the time required by both of them to attain the thermal equilibrium state. In Table 1 some typical values of G are given for different metals, it is clear that these values are large. Criterion (19) reveals that, in the considered framework, other slab properties such as the film thickness L, electron gas thermal conductivity k_e and electron gas thermal capacity C_e do not play any role in controlling the state of thermal equilibrium or the necessity of transition from the macroscopic model to the microscopic one.

Table 1 shows the ranges of angular frequency $\bar{\omega}$ beyond which using the microscopic heat conduction model is essential in metallic slabs made of different metals.

3. Results and discussion

Figs. 1 and 2 show the spatial and temporal temperature distributions for electron gas and solid lattice, respectively. It is clear from both figures that fluctuations in temperature disappear as we move far from the boundary. This implies that there is a limited thermal penetration depth for the fluctuating boundary-heating source. Comparing Figs. 1 and 2 reveals that the

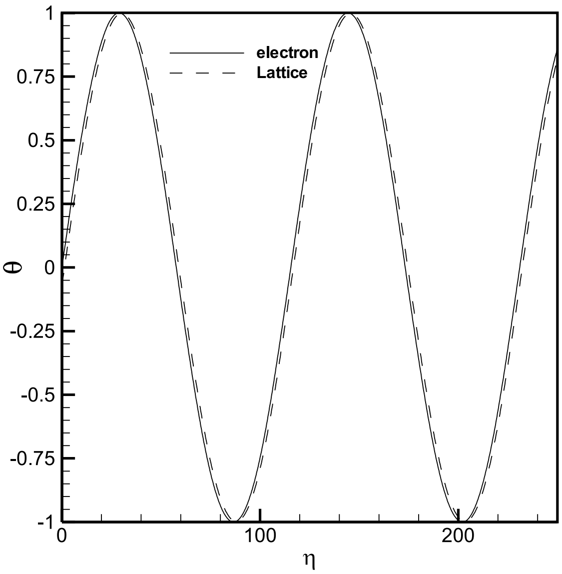

Fig. 3. Transient electron gas and solid lattice temperature distributions for Cu ($A = 124.352$, $C_R = 0.0061765$, $\bar{\omega} = 1 \times 10^9$, $\varepsilon = 1.0$, $\zeta = 1.0$).

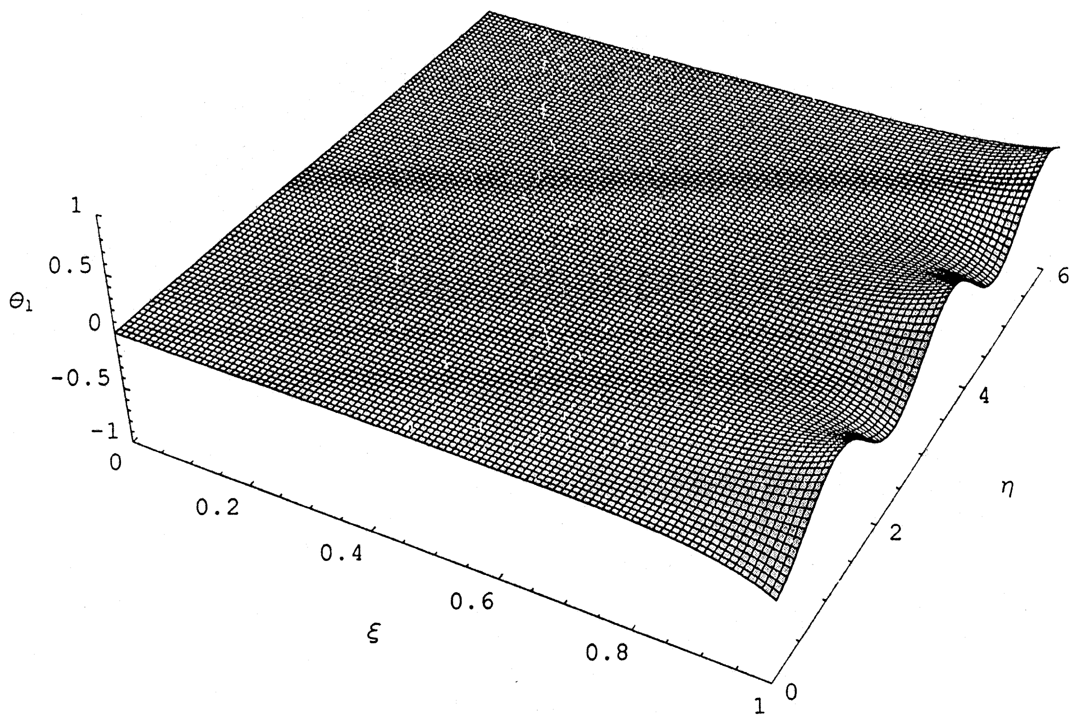

Fig. 2. Spatial and transient solid lattice temperature distribution for Cu ($A = 124.352$, $C_R = 0.0061765$, $\bar{\omega} = 5 \times 10^5$, $\varepsilon = 1.0$.

boundary thermal effect has a thicker thermal penetration depth in the electron gas than that in the solid lattice.

Figs. 3–6 show the harmonic variation in both electron gas and solid lattice temperatures for Cu at different frequencies. As predicted by the theoretical analysis, the deviation between both temperatures becomes significant at frequencies larger than 1×10^9 rad/s as shown in Table 1. Also, the phase-shift between both temperatures increases as ω increases and then reaches a fixed value.

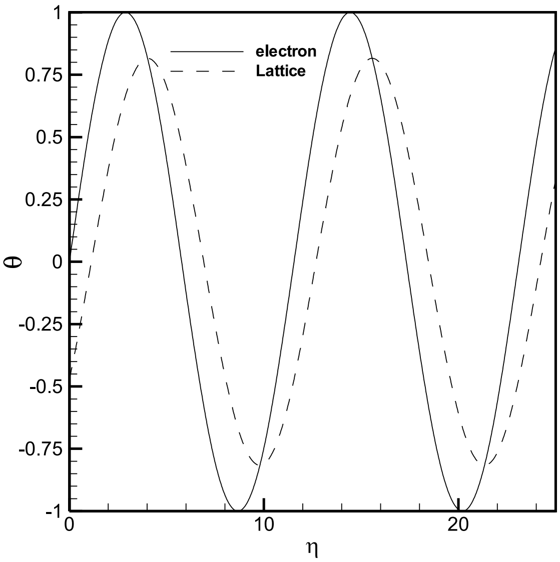

Fig. 4. Transient electron gas and solid lattice temperature distribution for Cu ($A = 124.352$, $C_R = 0.0061765$, $\bar{\omega} = 1 \times 10^{10}$, $\varepsilon = 1.0$, $\zeta = 1.0$).

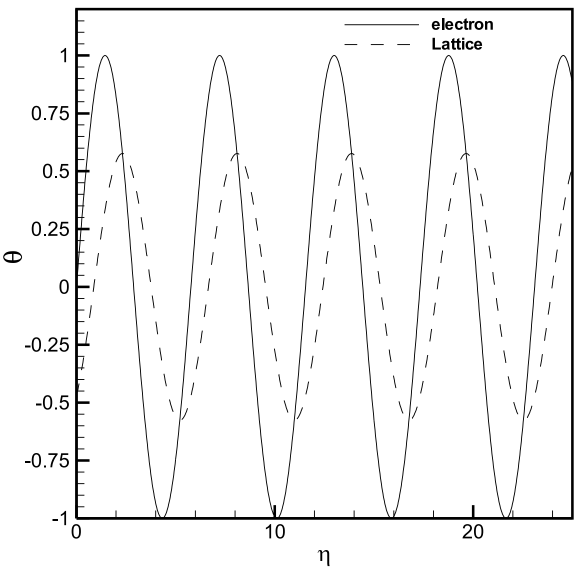

Fig. 5. Transient electron gas and solid lattice temperature distribution for Cu ($A = 124.352$, $C_R = 0.0061765$, $\bar{\omega} = 2 \times 10^{10}$, $\varepsilon = 1.0$, $\zeta = 1.0$).

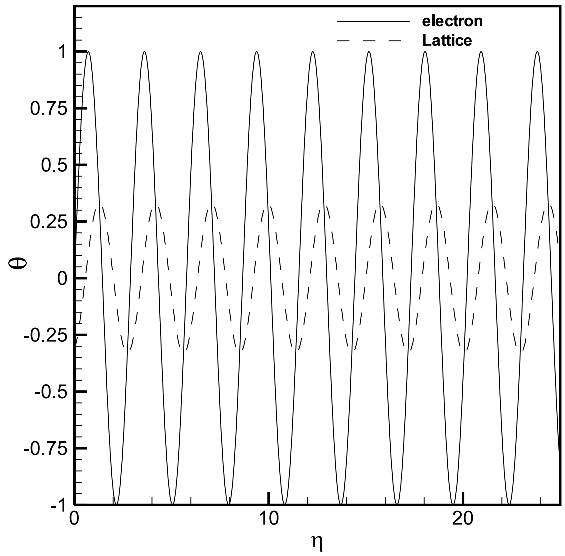

Fig. 6. Transient electron gas and solid lattice temperature distribution for Cu ($A = 124.352$, $C_R = 0.0061765$, $\bar{\omega} = 5 \times 10^{10}$, $\varepsilon = 1.0$, $\zeta = 1.0$).

The phase-shift δ as described by Eq. (15) is plotted in Fig. 7 as a function of ω/C_RA. Increasing ω/C_RA within its lower range leads to a sharp increase in δ. However, this increase becomes slower as ω/C_RA increases and then δ reaches an asymptotic value of 1.5708 rad.

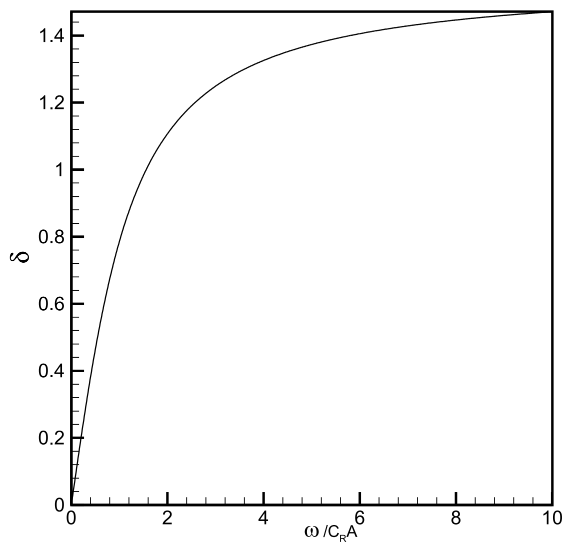

Fig. 7. Variation of the phase-shift between the electron gas and solid lattice temperature as a function of ω/C_RA.

Owing to Eq. (19), it is clear that the phase-shift becomes small as $\bar{\omega}$ and C_l decrease and as G increases. Any parameter that shortens the time required by the lattice to exchange energy with electron gas leads to a reduction in the phase-shift between the electron gas and the solid lattice temperatures.

The deviation between electron gas and solid lattice temperatures as a function of η—in the middle of the film—is shown in Fig. 8 for Cu and in Fig. 9 for Ag. The two figures show that the deviation $|\theta_e - \theta_l|$ becomes significant for $\bar{\omega} > 1 \times 10^9$ rad/s and this is in a good agreement with the predictions of Table 1.

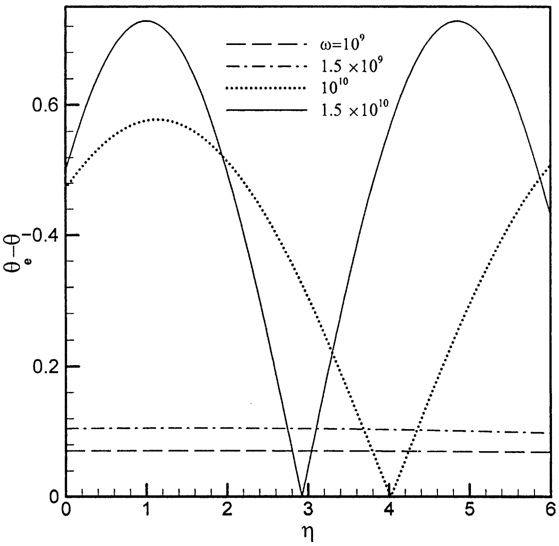

Fig. 8. Transient behavior of the temperature differences $\theta_e - \theta_l$ at different $\bar{\omega}$ for Cu ($A = 124.352$, $C_R = 0.0061765$, $\varepsilon = 1.0$, $\zeta = 1.0$).

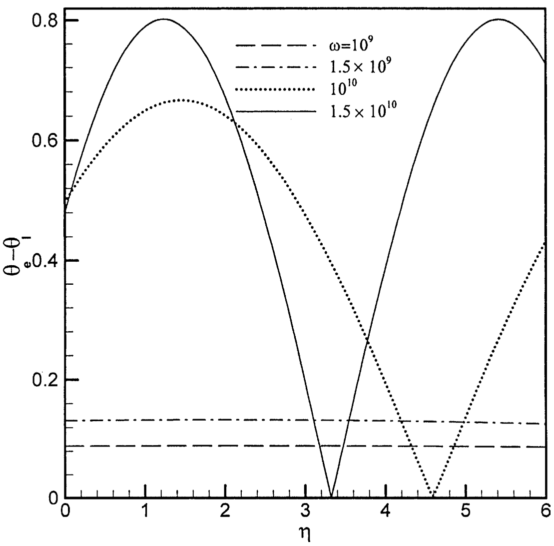

Fig. 9. Transient behavior of the temperature differences $\theta_e - \theta_l$ at different $\bar{\omega}$ for Ag ($A = 124.352$, $C_R = 0.0061765$, $\varepsilon = 1.0$, $\zeta = 1.0$).

4. Conclusion

The validity of using the microscopic parabolic heat conduction model under the effect of a high frequency fluctuating boundary heating source is investigated. It is found that the microscopic heat conduction model must be used if $\omega/C_R A > 0.1$ on a dimensionless basis or $\bar{\omega}C_l/G > 0.1$ on a dimensional basis. For $\bar{\omega}C_l/G < 0.1$, the difference and the phase-shift between θ_e and θ_l may be neglected and one may assume that $\theta_e \approx \theta_l$. The phase-shift between the electron gas and the solid lattice temperatures is found to be $\tan^{-1}(\omega/C_R A)$. This phase-shift reaches a fixed value of 1.5708 rad at very large values of $\omega/C_R A$ or $\bar{\omega}C_l/G$. Regarding the frequency $\bar{\omega}$, it is found that using the microscopic heat conduction model is essential when $\bar{\omega} > 1 \times 10^9$ rad/s for most metallic films regardless the layer thickness.

References

[1] D.Y. Tzou, in: Macro-to-Microscale Heat Transfer—The Lagging Behavior, Taylor and Francis, New York, 1997, pp. 1–64.

[2] T.Q. Qiu, C.L. Tien, Short-pulse laser heating on metals, Int. J. Heat Mass Transfer 35 (1992) 719–726.

[3] T.Q. Qiu, C.L. Tien, Heat transfer mechanism during short-pulse laser heating of metals, ASME J. Heat Transfer 115 (1993) 835–841.

[4] S.L. Anisimov, B.L. Kapeliovich, T.L. Perelman, Electron emission from metal surfaces exposed to ultrashort laser pulses, Sov. Phys. JETP 39 (1974) 375–377.

[5] J.G. Fujimoto, J.M. Liu, E.P. Ippen, Femtosecond laser interaction with metallic tungsten and non-equilibrium electron and lattice temperature, Phys. Rev. Lett. 53 (1984) 1837–1840.

[6] D.Y. Tzou, A unified field approach for heat conduction from macro- to microscales, J. Heat Transfer 117 (1995) 8–16.

[7] M.A. Al-Nimr, V.S. Arpaci, The thermal Behavior of thin metal films in the hyperbolic two-step model, Int. J. Heat Mass Transfer 43 (11) (2000) 2021–2028.

[8] M.A. Al-Nimr, V.S. Arpaci, Picosecond thermal pulses in thin metal films, J. Appl. Phys. 85 (5) (1999) 2517–2521.

[9] M.A. Al-Nimr, S. Masoud, Non-equilibrium laser heating of metal films, ASME J. Heat Transfer 119 (1997) 188–190.

[10] M.A. Al-Nimr, Heat transfer mechanisms during laser heating of thin metal films, Int. J. Thermophys. 18 (5) (1997) 1257–1268.

[11] M.A. Al-Nimr, O.M. Haddad, V.S. Arpaci, Thermal behavior of metal films—a hyperbolic two-step model, Heat Mass Transfer 35 (6) (1999) 459–464.

[12] T.Q. Qiu, C.L. Tien, Femtosecond laser heating of multilayered metals—I Analysis, Int. J. Heat Mass Transfer 37 (1999) 2789–2797.
[13] S. Kumar, M. Mitra, Microscale aspects of thermal radiation transport and laser applications, Adv. Heat Transfer 33 (1999) 287–294.
[14] M.A. Al-Nimr, S. Kiwan, Effect of thermal losses on the microscopic two-step heat conduction model, Int. J. Heat Mass Transfer 44 (2001) 1013–1018.
[15] S. Kiwan, M.A. Al-Nimr, Effect of radiative losses of the parabolic two-step heat conduction model, Jpn. J. Appl. Phys. 39 (2000) 4245–4248.